JOURNAL OF GUIDANCE, CONTROL, AND DYNAMICS
Vol. 29, No. 3, May–June 2006

Improved Indirect Method for Air-Vehicle Trajectory Optimization

Roger L. Barron*
Stanardsville, Virginia 22973
and
Cleon M. Chick III†
Charlottesville, Virginia 22903

An improved indirect method is presented for air-vehicle vertical-plane, two-point boundary-value trajectory optimization. The performance index is related to minimizing an integral weighted sum of quadratic terms in aerodynamic angle and propulsive thrust, modified to exclude all penalties associated with non-maneuvering flight. For this index, costate rates are constants if the dynamic model is continuous, assuring costate system stability, increasing radii of convergence in costate initializations, and facilitating propagation of costates. A multimodal, four-dimensional search initializes costates using predictive trajectory shooting. Multiple modes of the costate space are investigated in the search via simultaneous, parallel threads of computation. Within each thread, trial variances are adjusted adaptively to find a modal region of global quality and converge rapidly toward its best point. Costate-rate adaptation refines the initialization and subsequently provides compensation for identifiable changes in system parameters. Collocated analytical solutions, polynomial networks, and neural models are not used. Simulation results are presented for ascent and descent maneuvers of a notional unmanned air vehicle.

Nomenclature

$b_{10}, \ldots, b_{53}$	=	coefficients within costate differential equations
C_A	=	axial force coefficient
C_{N_α}	=	slope of normal force coefficient relative to α
$f_1, \ldots, f_5$	=	anholonomic subsidiary conditions
g	=	acceleration of gravity
h	=	altitude above mean sea level
K_1, K_2	=	reciprocals of constant Lagrange multipliers
m, m_{loss}	=	vehicle mass, mass loss during maneuver
$\dot{m}_T$	=	thrust-specific mass-flow rate
n	=	iteration number in search thread
Q_1, Q_2, Q_3	=	penalty weights in search score function
$\bar{q}$	=	dynamic pressure
T	=	thrust
$t, t_0, t_a, t_f, t_i, t_s, t_{\text{go}}$	=	time, time at start of trajectory, effective time of costate rate adaptation, final time, midmaneuver initial time, effective time of costate initialization, time remaining
u	=	horizontal component of velocity
V	=	resultant velocity magnitude
v	=	vertical component of velocity
x	=	horizontal distance
α	=	aerodynamic angle of attack
γ	=	flight-path climb angle
Δt	=	simulation integration interval
Δt_a	=	costate-rate adaptation interval
η_1, η_2	=	$V\cos\theta$, $V\sin\theta$
θ	=	pitch attitude of zero-lift axis relative to horizontal
$\lambda_1, \ldots, \lambda_5$	=	time-dependent Lagrange multipliers (costates)
ρ	=	atmosphere density
ψ	=	search score

Subscripts

m	=	trim value for minimum steady-state thrust required
tr	=	trim value for externally prescribed V

I. Introduction

TRAJECTORY optimization is important in air-vehicle development, operations planning, airspace traffic management, and in-flight guidance. Two-point boundary-value (TPBV) dynamic trajectory optimization is appropriate for precise, fuel-efficient, altitude and route changes as part of airspace management and for maneuvers associated with intercepts, landings, formation flight, endoatmospheric ascent into orbit, and reentry. A numerical search process is necessary to obtain solutions for such applications because air-vehicle equations of motion are highly nonlinear. The search generally involves multiple predictive calculations of opposite-boundary states, a procedure known as multiple shooting.

A direct method of solution typically treats point-by-point values of vehicle control variables, such as angle-of-attack α and thrust T, or any suitable set of basis functions that relate to variations of the controls with time. These become the search independent variables, the objective being to extremize a utility function involving trajectory errors and costs of control. An indirect method, if associated with the calculus of variations, transforms the TPBV trajectory problem into one of numerical search for appropriate values of costates (time-varying Lagrange multipliers) at a trajectory boundary. The states and costates at a boundary determine the trajectory uniquely in the absence of disturbances and unforeseen vehicle or atmosphere changes.

TPBV solution methods require fast and reliable search convergence, particularly if online solutions are contemplated. However, the search spaces, whether for direct or indirect solutions, are generally multimodal and nonunique and usually have small radii of convergence, and such can place a premium on estimating good

Received 23 February 2005; revision received 8 September 2005; accepted for publication 4 October 2005.

*Independent Consultant, 7593 Celt Road. Senior Member AIAA.
†Independent Consultant, 1623B Grove Street Extended.

first-iterate parameter vectors. In that connection various investigators have studied homotopy analysis, analytical collocation, polynomial networks, and/or neural modeling. Additionally, there have been efforts to improve the search engines themselves.

This paper presents an improved indirect method for air-vehicle TPBV trajectory optimization that incorporates two primary developments:

First, a modified integral performance index is specified that leads to minimization of propulsive effort and the dissipative effects of air resistance, which are defined relative to steady-state, minimum-thrust-required, trimmed flight for the time-varying values of altitude h, velocity V, climb angle γ, and vehicle mass m along the extremal path. The modified index penalizes only the incremental effort required by a maneuver and not the effort involved in sustaining minimum-thrust-required static equilibrium. (A null costate vector is associated with maintenance of this trimmed condition.) For the modified index, costate time derivatives are found via the calculus of variations to be constants if the system dynamic model has no discontinuities such as can result from vehicle staging or impairment. Constant rates assure stability of the costate system, thereby increasing radii of convergence in costate initialization searches, and facilitate propagation of costates between time boundaries. With costate stability, trajectory behavior is not overly sensitive to small changes in initial costates. Previously, indirect methods sometimes required convergence to a precision of many significant figures, and often evidenced bifurcation of trajectory responses and other forms of system chaotic behavior for minute costate changes.

Second, a probabilistically controlled parallel-computation random search has been developed that rapidly solves the multimodal, four-dimensional costate initialization problem for vertical-plane trajectories. The first iterate for this search is arbitrary and does not require help from collocated analytical solutions, polynomial networks, or neural models. The probability distribution for successive trials is centered on the location of the current best trial. An important characteristic of the search algorithm is its trial-variance control, which opens the search with large trial variances and gradually shrinks the variances as the search progresses. The algorithm investigates multiple modes of the search space via simultaneous, parallel threads of computation. The first thread to produce an iterate that satisfies a final boundary acceptance criterion (based on predicted final position; velocity; and, indirectly, fuel consumption) returns that iterate as the initialization result.

In the mid 1950s an F-104 was flown to a world altitude record while piloted manually along a predetermined optimum Mach vs altitude schedule. Development of this schedule had required painstaking cut-and-try searches by analysts seeking values of initializing costates for three sequential trajectory segments. The F-104 program and other successes drew attention to the potential of trajectory optimization via the calculus of variations. Later, steepest-descent searches were investigated for costate initialization, but lacked necessary multimodal capabilities. A perception gradually took root that indirect methods are awkward and have little future for real-time solutions. Except for studies of the use of polynomial networks and neural models for costate initialization,[1–6] modern research interest has turned largely toward direct methods, which also can lead to multi-modal search problems.

Much of the recent literature on trajectory optimization relates to endoatmospheric closed-loop guidance for purposes of orbital insertion, reentry, and landing.[6–13] Direct methods dominate that work, and current emphasis is placed on use of collocated solutions as first iterates in trajectory parameter searches. Polynomial networks and neural models continue to receive attention, but must be synthesized using a library of optimum TPBV solutions, raising questions of how those solutions should be obtained and how representative the library will be.

In Ref. 14, a modification of one-dimensional costate differential equations is investigated that promotes their stability (although with some sacrifice in optimality), but its approach is difficult to apply to the linked differential equations in problems of higher dimensionality.

In Refs. 15–20, parameter space search techniques relevant to the present study are dealt with specifically.

II. One-Dimensional Motivational Example

To illustrate the selection of performance criteria for indirect method variational calculus solutions, consider the one-dimensional nonlinear system discussed in Ref. 16,

$$\dot{V} + a_2 V^2 = bT \tag{1}$$

$$\dot{x} = V \tag{2}$$

where V is velocity, x is displacement, T is thrust, and a_2 and b are assumed to be positive constants. Take as the performance criterion to be minimized

$$\int_{t_0}^{t_f} F(T, V, \dot{V}, \dot{x})\, \mathrm{d}t \tag{3}$$

If F is written as[16]

$$F = T^2/K + \lambda_1\left(\dot{V} + a_2 V^2 - bT\right) + \lambda_2(\dot{x} - V) \tag{4}$$

wherein K is a positive constant and λ_1 and λ_2 are the costates, the applicable Euler–Lagrange (E–L) first-variation necessary conditions (see Ref. 21) yield the governing relationships shown in the first row (case 1) of Table 1. Thus, for the conventional performance index used in case 1, $\dot{\lambda}_1 = 2a_2 V\lambda_1 - \lambda_2$, λ_2 is constant, $T = bK\lambda_1/2$, and it is obvious that the $\dot{\lambda}_1$ costate differential equation is unstable for $V > 0$.

Three modified performance indices that lead to stable behavior of the costate system are also summarized in Table 1. For these it is seen by inspection that $\dot{\lambda}_1$ is constant. In case 2, an isoperimetric integral of $M\dot{\lambda}_1^2$ is added to the index, M being a positive-definite, constant Lagrange multiplier, so that the index penalizes nonzero values of $\dot{\lambda}_1$. The λ_1 E–L condition now requires that $\dot{\lambda}_1$ be a constant, specifically $2a_2 V(t')\lambda_1(t') - \lambda_2$, where t' is any discrete time $t_0 \le t' \le t_f$. (In Table 1, $t' = t_0$.) Note that $\dot{\lambda}_1$ is a different constant when propagating forward in time than when propagating backward, unless $a_2 = 0$. The costate system for case 2 is clearly stable. In case 3, the static equilibrium value of T, that is, $a_2 V^2/b$, is subtracted from T in the quadratic guidance effort penalty. Now the criterion penalizes perturbations of thrust relative to static equilibrium, and

Table 1 T, $\dot{\lambda}_1$, and λ_2 from E–L conditions applied to four performance indices

Case	Criterion Integrand[a]	T	$\dot{\lambda}_1$	λ_2
1	$T^2/K + \sum \lambda_n f_n$	$bK\lambda_1/2$	$2a_2 V\lambda_1 - \lambda_2$	Constant
2	$T^2/K + M\dot{\lambda}_1^2 + \sum \lambda_n f_n$	$bK\lambda_1/2$	$2a_2 V_i \lambda_{1_i} - \lambda_2$	Constant
3	$(T - a_2 V^2/b)^2/K + \sum \lambda_n f_n$	$bK\lambda_1/2 + a_2 V^2/b$	$-\lambda_2$	Constant
4	$(T - a_2 V^2/b)^2/K + M\dot{\lambda}_1^2 + \sum \lambda_n f_n$	$bK\lambda_1/2 + a_2 V^2/b$	$-\lambda_2$	Constant

[a] $\sum \lambda_n f_n = \lambda_1(\dot{V} + a_2 V^2 - bT) + \lambda_2(\dot{x} - V)$.

one obtains $\dot{\lambda}_1 = -\lambda_2 = \text{constant}$ (without the $M\dot{\lambda}_1^2$ penalty in the integrand), and so again the costate system is stable. The velocity is not specified, and if V changes for any reason, thrust will tend to change to a new (trim) equilibrium level. Case 4 combines the two modifications in a single performance index. Results for cases 3 and 4 are identical, but the combined index of case 4 has utility for more complex applications. Cases 2–4 provide stabilization of the costate system. It is particularly significant that a classical T^2 penalty does not provide assurance of costate stability in this example unless the integrand is augmented by a $\dot{\lambda}^2$ penalty.

The general t_f transversality condition[21] for the one-dimensional system is

$$(F_{\dot{T}})_f(\delta T_f - \dot{T}_f\delta t_f) + (F_{\dot{V}})_f(\delta V_f - \dot{V}_f\delta t_f) + (F_{\dot{x}})_f(\delta x_f - \dot{x}_f\delta t_f) + \left(F_{\dot{\lambda}_1}\right)_f\left(\delta\lambda_{1_f} - \dot{\lambda}_{1_f}\delta t_f\right) + \left(F_{\dot{\lambda}_2}\right)_f\left(\delta\lambda_{2_f} - \dot{\lambda}_{2_f}\delta t_f\right) + F_f\delta t_f = 0 \quad (5)$$

and if t_f is a fixed time, that is, $\delta t_f = 0$, this condition reduces to $\lambda_{1_f}\delta V_f + \lambda_2\delta x_f = 0$ because $(F_{\dot{T}})_f = (F_{\dot{\lambda}_1})_f = (F_{\dot{\lambda}_2})_f = 0$ and M may be set to an arbitrarily small value. Thus, if V_f and x_f are both specified a priori, $\delta V_f = \delta x_f = 0$ and λ_{1_f} and λ_2 are free (unaffected by the transversality requirement). However, if either V_f or x_f is specified, but not both, λ_2 must be zero if V_f is specified, and λ_{1_f} must be zero if x_f is specified.

III. Two-Dimensional Trajectory Optimization

A. Equations of Motion

Nonrotating Cartesian coordinates are used because air-path coordinates can introduce inherent instability within the system of costate differential equations. In the normal Earth-fixed axis system,[22] given subsonic motion restricted to a vertical plane with a flat, nonrotating Earth and constant acceleration of gravity, the force-balance equations, written in the form of dynamic constraints f_1 and f_2, are

$$f_1 = \dot{u} - \left[\left(T - C_1\rho V^2\right)\eta_1 - C_2\rho V^2\alpha\eta_2\right]/(mV) = 0 \quad (6)$$

$$f_2 = \dot{v} + g - \left[\left(T - C_1\rho V^2\right)\eta_2 + C_2\rho V^2\alpha\eta_1\right]/(mV) = 0 \quad (7)$$

C_1 and C_2 are defined as $C_A S/2$ and $C_{N_\alpha} S/2$, respectively, and the nondimensional force coefficients C_A and C_{N_α} are here assumed to be constant, although in practice they may also be functions of α, h, Mach number, and other variables. S is the reference area, and thrust is assumed to act along the zero-lift axis. Effects of quasi-steady winds and random gusts are not considered in this paper. Although in actuality the dynamic responses of α and T to guidance commands are not instantaneous, they are assumed to be so in the present study.

In Eqs. (6) and (7), η_1 and η_2 are defined as

$$\eta_1 = V\cos(\gamma + \alpha) = u\cos\alpha - v\sin\alpha \quad (8)$$

$$\eta_2 = V\sin(\gamma + \alpha) = u\sin\alpha + v\cos\alpha \quad (9)$$

where $V = \sqrt{(u^2 + v^2)}$ and $\gamma = \tan^{-1}(v/u)$.

The quantity $(T - C_1\rho V^2)$ is the net axial force, and the normal force is modeled as $C_2\rho V^2\alpha$. In this paper, α is restricted to the range ± 30 deg. A trigonometric relationship[23] could be used to express the normal force with greater generality.

The kinematic constraints are

$$f_3 = \dot{x} - u = 0 \quad (10)$$

$$f_4 = \dot{h} - v = 0 \quad (11)$$

and the mass rate balance equation is

$$f_5 = \dot{m} - \dot{m}_T T = 0 \quad (12)$$

in which $\dot{m}_T$ is assumed to be a constant thrust-specific mass-flow rate ($\dot{m}_T < 0$).

If maximum altitude is restricted to 12,000 m, the U.S. standard atmosphere density (which itself is subject to errors of as much as $\pm 15\%$ depending on time and location) may be approximated within $\pm 3\%$ by the exponential function

$$\rho = \rho_{\text{SL}}(1 - Bh/\theta_{\text{SL}})^{(g/\text{RB}-1)} \quad (13)$$

in which $\rho_{\text{SL}} = 1.225$ kg/m^3 is the density at sea level, $B = 0.0065$ K/m is the temperature lapse rate with altitude, $R = 287.053$ m^2/s^2/K is the gas constant, and $\theta_{\text{SL}} = 288.15$ K is the atmosphere absolute temperature at sea level. The gradient of $\rho(h)$ is

$$\rho_h = \rho(B - g/R)/(\theta_{\text{SL}} - Bh) \quad (14)$$

B. Trim Conditions

A starting trim condition for vertical-plane trajectories may be that which minimizes the steady-state thrust required to maintain force balance at given m_0, h_0, and γ_0. When trimmed, $\dot{u}_0 = \dot{v}_0 = 0$. One may solve iteratively[24] for α and V (here denoted α_{m_0} and V_{m_0}) that provide minimum T_{m_0}. For small α the iteration involves:

$$\alpha_{m_0} = \left[m_0 g\cos\left(\gamma_0 + \alpha_{m_0}\right)\right]\Big/\left(C_2\rho_0 V_{m_0}^2\right) \quad (15)$$

$$V_{m_0}^2 = m_0 g\left[-\sin\left(\gamma_0 + \alpha_{m_0}\right) + \sqrt{\sin^2\left(\gamma_0 + \alpha_{m_0}\right) + (4C_2/C_1)\cos^2\left(\gamma_0 + \alpha_{m_0}\right)}\right]\Big/(2C_2\rho_0) \quad (16)$$

after which

$$T_{m_0} = C_1\rho_0 V_{m_0}^2 + m_0 g\sin\left(\gamma_0 + \alpha_{m_0}\right) \quad (17)$$

The trim solution for an externally prescribed m, h, γ, and V may be obtained by numerical iteration of

$$\alpha_{\text{tr}} = [mg\cos(\gamma + \alpha_{\text{tr}})]\Big/\left(C_2\rho V^2\right) \quad (18)$$

after which

$$T_{\text{tr}} = C_1\rho V^2 + mg\sin(\gamma + \alpha_{\text{tr}}) \quad (19)$$

An alternative starting trim solution for unthrusted cases is that for maximum steady-state glide range. To maximize the lift/drag ratio,[23] C_{L_W}/C_{D_W}, where $C_{L_W} = -C_A\sin\alpha + C_N\cos\alpha$ and $C_{D_W} = C_A\cos\alpha + C_N\sin\alpha$, if C_A and C_{N_α} are constants, the best α_{m_0} is the smallest positive root of the equation

$$2C_2(C_2 - C_1)\alpha_{m_0}\sin\alpha_{m_0} + \left[\alpha_{m_0}^2 - C_1(1 + C_1/C_2)\right]\cos 2\alpha_{m_0} = 0 \quad (20)$$

When this equation is solved iteratively, a suitable first approximation to the desired root is

$$\alpha_{m_0} = \sqrt{C_1(1 + C_1/C_2)/[1 + 4(C_2 - C_1)]} \quad (21)$$

Note that α_{m_0} for maximum steady-state glide range is a function solely of vehicle aeroparameters. With α_{m_0} known, the values of u_{m_0} and v_{m_0} and γ_{m_0} and V_{m_0} are readily computed from the equations of motion with $\dot{u}_0$ and $\dot{v}_0$ set to zero.

C. Performance Index

The two-dimensional, TPBV performance index that is to be minimized is, when expressed in Lagrange form,

$$\int_{t_0}^{t_f} F(\alpha, T, u, \dot{u}, v, \dot{v}, x, \dot{x}, h, \dot{h}, m, \dot{m}, \lambda_1, \ldots, \lambda_5, \dot{\lambda}_1, \ldots, \dot{\lambda}_5)\,\mathrm{d}t \quad (22)$$

in which the costates, $\lambda_1, \ldots, \lambda_5$, are, in general, functions of time. The final time t_f is here treated as fixed, and the specific integrand used is

$$F = \Lambda_1 + \frac{(\alpha - \sigma_1\alpha_{\text{tr}})^2}{K_1} + \frac{(T - \sigma_2 T_{\text{tr}})^2}{K_2} + \sum_{n=1}^{5}\left(\lambda_n f_n + M_n \dot{\lambda}_n^2\right) \tag{23}$$

where $f_1, \ldots, f_5$ are given by Eqs. (6–12) and Λ_1, K_1, K_2, and $M_1, \ldots, M_5$ are positive constants. Λ_1 pertains only to minimum-time solutions and is set to zero in the present application. The constants σ_1 and σ_2 are 0, 1 switches (constant at zero or one) that provide alternative formulations for confirmation of the theory; these are both unity in the present application.

The parameters α_{tr} and T_{tr} in Eq. (23) are the instantaneous trim values from Eqs. (18) and (19), which have the following nonzero partial derivatives required later in derivation of the costate differential equations:

$$\alpha_{\text{tr}_u} = -mg\left(\cos\alpha_{\text{tr}} - 3\eta_{1_{\text{tr}}} u/V^2\right)/\left[1 + mg\eta_{2_{\text{tr}}}/\left(C_2\rho V^3\right)\right]/\left(C_2\rho V^3\right) \tag{24}$$

$$\alpha_{\text{tr}_v} = -mg\left(\sin\alpha_{\text{tr}} + 3\eta_{1_{\text{tr}}} v/V^2\right)/\left[1 - mg\eta_{2_{\text{tr}}}/\left(C_2\rho V^3\right)\right]/\left(C_2\rho V^3\right) \tag{25}$$

$$\alpha_{\text{tr}_h} = -mg\rho_h[\cos(\gamma + \alpha_{\text{tr}})]/\left(C_2\rho^3 V^3\right) \tag{26}$$

$$\alpha_{\text{tr}_m} = g[\cos(\gamma + \alpha_{\text{tr}})]/\left(C_2\rho V^2\right) \tag{27}$$

$$T_{\text{tr}_u} = 2C_1\rho u + mg[\cos(\gamma + \alpha_{\text{tr}})]\left(\alpha_{\text{tr}_u} - v/V^2\right) \tag{28}$$

$$T_{\text{tr}_v} = 2C_1\rho v + mg[\cos(\gamma + \alpha_{\text{tr}})]\left(\alpha_{\text{tr}_v} + u/V^2\right) \tag{29}$$

$$T_{\text{tr}_h} = C_1\rho_h V^2 + mg[\cos(\gamma + \alpha_{\text{tr}})]/\left(C_2\rho V^2\right) \tag{30}$$

$$T_{\text{tr}_m} = g\sin(\gamma + \alpha_{\text{tr}}) \tag{31}$$

D. Angle-of-Attack and Thrust Commands

The E–L first-variation necessary conditions[21] for $\alpha(t)$ and $T(t)$ over the interval $t_i \le t \le t_f$ reduce to $F_\alpha = 0$ and $F_T = 0$, respectively. Casual application of these conditions would produce coupled, nonlinear equations for α and T, leading to serious uniqueness problems. An alternative is to linearize the command functions relative to a moving operating point (α_{tr}, T_{tr}).

First, for the $T(t)$ manipulable (control) variable, the general E–L condition is readily shown to yield

$$2(T - \sigma_2 T_{\text{tr}})/K_2 - (\lambda_1\eta_1 + \lambda_2\eta_2)/(mV) - \lambda_5\dot{m}_T = 0 \tag{32}$$

which provides

$$T = \sigma_2 T_{\text{tr}} + K_2[(\lambda_1\eta_1 + \lambda_2\eta_2)/(mV) - \lambda_5\dot{m}_T]/2 \tag{33}$$

and for the $\alpha(t)$ freedom, the general E–L condition is

$$2(\alpha - \sigma_1\alpha_{\text{tr}})/K_1 - \lambda\left\{\left[(T - A)\eta_{1_\alpha} + N_\alpha\left(\eta_2 + \alpha\eta_{2_\alpha}\right)\right]/(mV)\right\} - \lambda_2\left\{\left[(T - A)\eta_{2_\alpha} - N_\alpha\left(\eta_1 + \alpha\eta_{1_\alpha}\right)\right]/(mV)\right\} = 0 \tag{34}$$

where $A = C_1\rho V^2$ and $N_\alpha = C_2\rho V^2$. However, $\eta_{1_\alpha} = -\eta_2$, and $\eta_{2_\alpha} = \eta_1$, so Eq. (34) becomes

$$\alpha = \sigma_1\alpha_{\text{tr}} + K_1\{\lambda_1[-(T - A)\eta_2 + N_\alpha(\eta_2 + \alpha\eta_1)] + \lambda_2[(T - A)\eta_1 - N_\alpha(\eta_1 - \alpha\eta_2)]\}/(2mV) \tag{35}$$

From Eqs. (8) and (9), substituting the definition of pitch attitude, $\theta = \gamma + \alpha$, one has $\eta_1 = V\cos\theta$ and $\eta_2 = V\sin\theta$. For a small perturbation $\Delta\theta$ at t, $\Delta\theta = \Delta\alpha$ because γ cannot change in a zero time interval as can (considered on a trajectory-guidance timescale) α and T. Accordingly, for perturbations of α and T relative to trim, $\Delta\alpha = \alpha - \alpha_{\text{tr}} = \theta - \theta_{\text{tr}}$ and $\Delta T = T - T_{\text{tr}}$. Thus, from Eqs. (33) and (35)

$$T = \sigma_2 T_{\text{tr}} + \Delta T = \sigma_2 T_{\text{tr}} + K_2\{[\lambda_1\cos(\theta_{\text{tr}} + \Delta\alpha) + \lambda_2\sin(\theta_{\text{tr}} + \Delta\alpha)]/(mV) - \lambda_5\dot{m}_T\}/2 \tag{36}$$

$$\alpha = \sigma_1\alpha_{\text{tr}} + \Delta\alpha = \sigma_1\alpha_{\text{tr}} + K_1\{\lambda_1[-(T - A)\sin(\theta_{\text{tr}} + \Delta\alpha) + N_\alpha\sin(\theta_{\text{tr}} + \Delta\alpha) + N_\alpha(\alpha_{\text{tr}} + \Delta\alpha)\cos(\theta_{\text{tr}} + \Delta\alpha)] + \lambda_2[(T - A)\cos(\theta_{\text{tr}} + \Delta\alpha)\sin(\theta_{\text{tr}} + \Delta\alpha) + N_\alpha(\alpha_{\text{tr}} + \Delta\alpha)\sin(\theta_{\text{tr}} + \Delta\alpha)]\}/(2m) \tag{37}$$

If $\Delta\alpha$ is small

$$\cos(\theta_{\text{tr}} + \Delta\alpha) = \cos\theta_{\text{tr}} - \Delta\alpha\sin\theta_{\text{tr}} \tag{38}$$

$$\sin(\theta_{\text{tr}} + \Delta\alpha) = \sin\theta_{\text{tr}} + \Delta\alpha\cos\theta_{\text{tr}} \tag{39}$$

so that, defining

$$P_1 = \lambda_2\cos\theta_{\text{tr}} - \lambda_1\sin\theta_{\text{tr}} = [\lambda_2(u\cos\alpha_{\text{tr}} - v\sin\alpha_{\text{tr}}) - \lambda_1(v\cos\alpha_{\text{tr}} + u\sin\alpha_{\text{tr}})]/V \tag{40}$$

$$P_2 = \lambda_1\cos\theta_{\text{tr}} + \lambda_2\sin\theta_{\text{tr}} = [\lambda_1(u\cos\alpha_{\text{tr}} - v\sin\alpha_{\text{tr}}) - \lambda_2(v\cos\alpha_{\text{tr}} + u\sin\alpha_{\text{tr}})]/V \tag{41}$$

one has

$$T = \sigma_2 T_{\text{tr}} + \Delta T = \sigma_2 T_{\text{tr}} + K_2[(P_2 + P_1\Delta\alpha)/(mV) - \lambda_5\dot{m}_T]/2 \tag{42}$$

$$\alpha = \sigma_1\alpha_{\text{tr}} + \Delta\alpha = \sigma_1\alpha_{\text{tr}} + K_1[(T - A - N_\alpha)(P_1 - P_2\Delta\alpha) + N_\alpha(\alpha_{\text{tr}} + \Delta\alpha)(P_2 + P_1\Delta\alpha)]/(2m) \tag{43}$$

When Eqs. (42) and (43) are combined while the term in $(\Delta\alpha)^2$ is discarded,

$$\alpha = \sigma_1\alpha_{\text{tr}} + \Delta\alpha = \sigma_1\alpha_{\text{tr}} + K_1(\{\sigma_2 T_{\text{tr}} + K_2[(P_2 + P_1\Delta\alpha)/(mV) - \lambda_5\dot{m}_T]/2 - A - N_\alpha\}(P_1 - P_2\Delta\alpha) + N_\alpha[\alpha_{\text{tr}}P_2 + (\alpha_{\text{tr}}P_1 + P_2)\Delta\alpha])/(2m) \tag{44}$$

so that

$$\Delta\alpha = \frac{K_1}{2m}\left\{\left[\sigma_2 T_{\text{tr}} + \frac{K_2}{2}\left(\frac{P_2}{mV} - \lambda_5\dot{m}_T\right) - A - N_\alpha\right]P_1 + N_\alpha\alpha_{\text{tr}}P_2\right\} + \frac{K_1}{2m}\left\{\frac{K_2}{2}\left(\frac{P_1^2}{mV}\right) - \left[\sigma_2 T_{\text{tr}} + \frac{K_2}{2}\left(\frac{P_2}{mV} - \lambda_5\dot{m}_T\right) - A - N_\alpha\right]P_2 + N_\alpha(\alpha_{\text{tr}}P_1 + P_2)\right\}\Delta\alpha \tag{45}$$

which yields

$$\Delta\alpha = G_1/G_2 \tag{46}$$

where, if

$$G_0 = \sigma_2 T_{\text{tr}} + K_2[P_2/(mV) - \lambda_5\dot{m}_T]/2 - A - N_\alpha \tag{47}$$

then

$$G_1 = K_1(G_0 P_1 + N_\alpha\alpha_{\text{tr}}P_2)/(2m) \tag{48}$$

$$G_2 = 1 - K_1\left[K_2 P_1^2/(2mV) - G_0 P_2 + N_\alpha(\alpha_{\text{tr}}P_1 + P_2)\right]/(2m) \tag{49}$$

Under rare circumstances, $G_2 \to 0$, and care must be taken to avoid singularity of $\Delta\alpha$. One approach is to set very tight limits on $\Delta\alpha$ as G_2 approaches zero.

When $\Delta\alpha$ has been obtained, Eq. (33) may be used to compute T. However, if $T(t) = T_{\text{sch}}(t)$, scheduled independently of the optimization process, Eq. (45) becomes

$$\alpha = \sigma_1\alpha_{\text{tr}} + \Delta\alpha = \sigma_1\alpha_{\text{tr}} + K_1\{(T_{\text{sch}} - A - N_\alpha)(P_1 - P_2\Delta\alpha) + N_\alpha[\alpha_{\text{tr}}P_2 + (\alpha_{\text{tr}}P_1 + P_2)\Delta\alpha]\}/(2m) \quad (50)$$

and, in Eq. (46) for $\Delta\alpha$, the parameters G_1 and G_2 are replaced with

$$G_1' = K_1[(T_{\text{sch}} - A - N_\alpha)P_1 + N_\alpha\alpha_{\text{tr}}P_2]/(2m) \quad (51)$$

$$G_2' = 1 - K_1[-(T_{\text{sch}} - A - N_\alpha)P_2 + N_\alpha(\alpha_{\text{tr}}P_1 + P_2)]/(2m) \quad (52)$$

Because of physical limits in attainable $\dot\alpha$ and $\dot T$, and the assumption that $\Delta\alpha$ is small, one must limit the changes in α and T during each Δt interval between updates in the solutions, that is,

$$|\Delta\alpha|/\Delta t \le |\dot\alpha|_{\max} \quad (53)$$

$$|\Delta T|/\Delta t \le |\dot T|_{\max} \quad (54)$$

Moreover, α and T are subject to magnitude limits

$$\alpha_{\min} \le \alpha \le \alpha_{\max} \quad (55)$$

$$T_{\min} \le T \le T_{\max} \quad (56)$$

Whenever T is at a limit, Eqs. (51) and (52) should not be used for computation of $\Delta\alpha$.

E. Costate Differential Equations

The costate differential equations (CDEs) are obtained from the E–L necessary conditions applicable to the u, v, x, h, m, and $\lambda_1, \ldots, \lambda_5$ freedoms. It is readily shown that the first five of these equations have the generic form

$$\dot\lambda_j = b_{j0} + b_{j1}\lambda_1 + \cdots + b_{j5}\lambda_5 \qquad j = 1, \ldots, 5, \qquad t_i \le t \le t_f \quad (57)$$

in which

$$b_{j0} = \frac{\partial\left[\Lambda_1 + (\alpha - \sigma_1\alpha_{\text{tr}})^2/K_1 + (T - \sigma_2 T_{\text{tr}})^2/K_2\right]}{\partial z_j} \quad (58)$$

$$b_{jk} = \frac{\partial\left(\sum_k \lambda_k f_k\right)}{\partial z_j} \quad (59)$$

z_j being the jth element of $z = [u, v, x, h, m]^T$.

Derivation of the coefficients in the CDEs, which is tedious but straightforward and omitted here in the interest of brevity, yields

$$b_{10} = -2(\alpha - \sigma_1\alpha_{\text{tr}})\sigma_1\alpha_{\text{tr}_u}/K_1 - 2(T - \sigma_2 T_{\text{tr}})\sigma_2 T_{\text{tr}_u}/K_2 \quad (60)$$

$$b_{11} = \left[-\left(T - C_1\rho V^2\right)\eta_2 v/V^2 + 2C_1\rho\eta_1 u + C_2\rho\eta_3\alpha\right]/(mV) \quad (61)$$

$$b_{12} = \left[\left(T - C_1\rho V^2\right)\eta_1 v/V^2 + 2C_1\rho\eta_2 u + C_2\rho\eta_4\alpha\right]/(mV) \quad (62)$$

$$b_{13} = -1 \quad (63)$$

$$b_{14} = b_{15} = 0 \quad (64)$$

$$b_{20} = -2(\alpha - \sigma_1\alpha_{\text{tr}})\sigma_1\alpha_{\text{tr}_v}/K_1 - 2(T - \sigma_2 T_{\text{tr}})\sigma_2 T_{\text{tr}_v}/K_2 \quad (65)$$

$$b_{21} = \left[\left(T - C_1\rho V^2\right)\eta_2 u/V^2 + 2C_1\rho\eta_1 v - C_2\rho\eta_5\alpha\right]/(mV) \quad (66)$$

$$b_{22} = \left[-\left(T - C_1\rho V^2\right)\eta_1 u/V^2 + 2C_1\rho\eta_2 v + C_2\rho\eta_6\alpha\right]/(mV) \quad (67)$$

$$b_{23} = b_{25} = 0 \quad (68)$$

$$b_{24} = -1 \quad (69)$$

wherein

$$\eta_3 = 2u^2\sin\alpha + uv\cos\alpha + v^2\sin\alpha \quad (70)$$

$$\eta_4 = u^2\cos\alpha + uv\sin\alpha + 2v^2\cos\alpha \quad (71)$$

$$\eta_5 = 2u^2\cos\alpha - uv\sin\alpha + v^2\cos\alpha \quad (72)$$

$$\eta_6 = u^2\sin\alpha - uv\cos\alpha + 2v^2\sin\alpha \quad (73)$$

Moreover, $b_{3j} = 0$ for all j, whereas

$$b_{40} = -2(\alpha - \sigma_1\alpha_{\text{tr}})\sigma_1\alpha_{\text{tr}_h}/K_1 - 2(T - \sigma_2 T_{\text{tr}})\sigma_2 T_{\text{tr}_h}/K_2 \quad (74)$$

$$b_{41} = (C_1\eta_1 - C_2\eta_2\alpha)\rho_h V/m \quad (75)$$

$$b_{42} = (C_1\eta_2 + C_2\eta_1\alpha)\rho_h V/m \quad (76)$$

$$b_{43} = b_{44} = b_{45} = 0 \quad (77)$$

$$b_{50} = -2(\alpha - \sigma_1\alpha_{\text{tr}})\sigma_1\alpha_{\text{tr}_m}/K_1 - 2(T - \sigma_2 T_{\text{tr}})\sigma_2 T_{\text{tr}_m}/K_2 \quad (78)$$

$$b_{51} = \left[\left(T - C_1\rho V^2\right)\eta_1 - C_2\rho V^2\alpha\eta_2\right]/(m^2 V) \quad (79)$$

$$b_{52} = \left[\left(T - C_1\rho V^2\right)\eta_2 + C_2\rho V^2\alpha\eta_1\right]/(m^2 V) \quad (80)$$

$$b_{53} = b_{54} = b_{55} = 0 \quad (81)$$

The five remaining CDEs result from application of the E–L conditions for the $\lambda_1, \ldots, \lambda_5$ freedoms. These conditions require that

$$2M_j\ddot\lambda_j = \partial F/\partial\lambda_j = f_j, \qquad j = 1, \ldots, 5, \quad t_i \le t \le t_f \quad (82)$$

However, $f_j = 0$ for every j, and, therefore,

$$\dot\lambda_j = \dot\lambda_{j_c} = (\text{constant})_j, \qquad j = 1, \ldots, 5 \quad (83)$$

From Eqs. (57) and (83), one has at $t = t_i$

$$\dot\lambda_{1_c} = b_{10_i} + b_{11_i}\lambda_{1_i} + b_{12_i}\lambda_{2_i} - \lambda_3 \quad (84)$$

$$\dot\lambda_{2_c} = b_{20_i} + b_{21_i}\lambda_{1_i} + b_{22_i}\lambda_{2_i} - \lambda_{4_i} \quad (85)$$

$$\dot\lambda_{3_c} = 0\ (\lambda_3 = \text{constant}) \quad (86)$$

$$\dot\lambda_{4_c} = b_{40_i} + b_{41_i}\lambda_{1_i} + b_{42_i}\lambda_{2_i} \quad (87)$$

$$\dot\lambda_{5_c} = b_{50_i} + b_{51_i}\lambda_{1_i} + b_{52_i}\lambda_{2_i} \quad (88)$$

in which the subscript c emphasizes that these derivatives are constants.

Consider the ΔT and $\Delta\alpha$ command functions. If the costate vector is null, $\Delta T = \Delta\alpha = 0$. Thus, if $\sigma_1 = \sigma_2 = 1$, the guided vehicle receives trim commands $T = T_{\text{tr}}$ and $\alpha = \alpha_{\text{tr}}$ and, therefore, remains at or transitions to its steady-state trim.

Ideally, the CDEs are computed only at the start of a maneuver. If there is a change in the specified final states and/or specified final time before an existing maneuver is completed, or if reinitialization is needed because of system parameter change, a new two-point boundary-value solution involving the CDEs may be invoked. (As will be seen, the simpler process of costate-rate adaptation is usually a satisfactory substitute for reinitialization.)

F. Transversality Condition

This paper considers the fixed t_f form of the t_f transversality condition.[21] If t_f is fixed, $\delta t_f = 0$, and the condition becomes

$$\lambda_{1_f}\delta u_f + \lambda_{2_f}\delta v_f + \lambda_{3_f}\delta x_f + \lambda_{4_f}\delta h_f + \lambda_{5_f}\delta m_f + 2\sum_{j=1}^{5} M_j\dot\lambda_{j_f}\delta\lambda_{j_f} = 0 \quad (89)$$

Without loss of generality, $M_1, \ldots, M_5$ may be set to arbitrarily small, positive-definite values, such that the summation term in Eq. (89) is reduced to negligible influence on the transversality condition. Now, if the final values of the trajectory states are specified, leaving the maneuver fuel consumption (and, therefore, m_f) free (subject, indirectly, to optimization during the initialization search), one has

$$\delta u_f = \delta v_f = \delta x_f = \delta h_f = \lambda_{5_f} = 0 \tag{90}$$

which provide satisfaction of Eq. (89). From the requirement imposed on λ_{5_f} by Eq. (90),

$$\lambda_{5_i} = -(t_f - t_i)\dot{\lambda}_{5_c} = -(t_f - t_i)\left(b_{50_i} + b_{51_i}\lambda_{1_i} + b_{52_i}\lambda_{2_i}\right) \tag{91}$$

IV. Costate Numerical Searches

A. Costate Initialization Search

A costate initialization search algorithm can be linked with a trajectory simulation routine to null predicted final errors in h and v and simultaneously minimize a measure of fuel consumption. The initialization process must generally contend with multimodal, multidimensional, nonunique search spaces having small radii of convergence.

There is a considerable amount of literature on parameter space search,[15–20] but the problem of achieving rapid convergence in multimodal spaces with small radii of convergence remains challenging. With a systematic search, if the grid size is made sufficiently small to capture the desired solution, the number of search trials becomes unacceptably large. Steepest descent algorithms can converge rapidly (except in spaces of very high dimensionality), but become trapped on inferior minima in a multimodal space. Uniform random searches will converge to the global minimum with probability one; however, the number of trials required usually is unacceptably large. With control of search trial variances, a random search can be accelerated, but thereby loses its assured multimodal capability.

A fundamental difficulty in accelerating convergence is that as a search progresses it becomes less and less likely that subsequent trials will locate a superior mode because the relative hypervolume of regions that yield scores better than the current best becomes smaller and smaller in comparison to the total search space. Ultimately, there is an element of chance involved in finding a mode of global quality with a single-thread, accelerated random search. Use of parallel threads increases the odds that at least one thread will find and converge within a suitable mode.

In the proposed algorithm, each of 16 threads is permitted a maximum of 250 probabilistically controlled random predictive trials to find a promising mode in the search space and locate the approximate best point within that mode. Each thread endeavors to satisfy acceptability criteria that require (1) operation above stall speed, (2) maneuvering confined to specified altitude limits (zero to 12 km in this study), (3) no heading reversals, and (4) $|h_e| < 10$ m and $|v_e| < 0.5$ m/s, where h_e and v_e are predicted final errors in altitude and vertical velocity. The first thread that achieves success returns the four initialized costate values, λ_{1_i}, λ_{2_i}, λ_3, and λ_{4_i}. [The transversality condition, Eq. (95), provides λ_{5_i} as a function of λ_{1_i} and λ_{2_i}.] When the acceptability criteria have been satisfied, the remainder of the search is amenable to a predictive Newton type of adjustment for fine tuning via costate-rate adaptation.

At the beginning of a costate initialization search, a supervisory routine first computes the predicted score for the null-costate trajectory and passes this information to the parallel threads, which then proceed independently. Whenever an iterate within a thread is found to satisfy the above criteria (1), (2), and (3), a trajectory performance score is computed using the function

$$\psi = Q_1|h_e| + Q_2|v_e| + Q_3(m_i - m_f) \tag{92}$$

where Q_1, Q_2, and Q_3 are nonnegative penalty weights and $(m_i - m_f)$ is the predicted m_{loss} (a surrogate for predicted fuel consumption). The penalty weights in Eq. (92) are governed by logic that implements the truth system in Table 2.

Table 2 Penalty weight truth system

$\lvert h_e\rvert > 20$ m?	$\lvert v_e\rvert > 0.5$ m/s?	Q_1	Q_2	Q_3
No	No	0.01	3.0	0.3
No	Yes	0.01	9.0	0.3
Yes	No	0.04	3.0	0.3
Yes	Yes	0.01	9.0	0.3

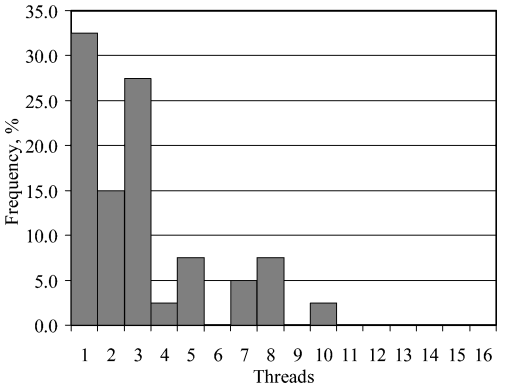

Fig. 1 Serial simulation results: parallel threads for initialization search convergence.

After the start, there is no sharing of costate vectors and scores between the multiple threads. Each thread uses its current best score, denoted ψ_{CB}, with its related costate vector to compute standard deviation $(\overline{\text{SD}})_n$ of the nth iteration from

$$(\overline{\text{SD}}_j)_n = (\lambda_j)_n \cdot (\overline{\text{SF}}_j)_n \cdot (\psi_{\text{CB}})_n \tag{93}$$

in which $(\lambda_j)_n$ is any of the four independent search variables and $(\overline{\text{SF}}_j)_n$ is the scale factor

$$(\overline{\text{SF}}_j)_n = 199/[99(n-1) + 199] \tag{94}$$

If $(\lambda_j)_n = 0$, it is replaced by 0.1 in Eq. (93).

The random trial perturbation at trial n is drawn from a normal distribution of mean zero and standard deviation dictated by Eq. (93). This perturbation is computed independently for each component of the costate vector, and the resulting perturbation vector is added to the current best costate vector (denoted λ_{CB}). Thus, for the jth costate at trial n,

$$(\lambda_j)_n = [(\lambda_{\text{CB}})_j)]_{n-1} + \text{N}[0, (\overline{\text{SD}}_j)_n], \qquad j = 1, \ldots, 4 \tag{95}$$

Within the preceding framework, each thread may be viewed in simplified terms as opening with a random four-dimensional multimodal exploration phase and closing with a random, partially four-dimensional, partially two-dimensional, mode characterization phase. The first phase lasts until five successful trials have been produced, or until $n = 80$, whichever occurs first. In this phase the search perturbations are relatively large, albeit gradually diminishing. In the second phase, the thread devotes approximately three-fourths of its activity to the use of two-dimensional subspace searching, and the remainder of its activity to searching in four dimensions. Moreover, in the second phase $(\overline{\text{SF}})_n$ becomes small as n continues to increase. For each trial in the second phase, a uniform random selection is made among eight options. Six of the options represent two-at-a-time combinations of the four independent variables, whereas the remaining two represent four-at-a-time perturbations.

With multiple threads running in parallel, the initialization search improves its odds of achieving an acceptable result. To evaluate the parallel search, serial simulations were performed in which the search was restarted and assigned a new random number sequence every 250 iterations. Figure 1 shows the histogram of results

obtained in 40 independent multiple-thread costate initializations, one-half representing 600-s ascents by the air vehicle from 2000 to 6000 m, and one-half representing 600-s descents from 6000 to 2000 m. The specified v_f for all cases was zero. The histogram reveals that a single thread was sufficient for 32.5% of the 40 cases, two threads for 47.5%, three threads for 75.0%, etc. Within the successful threads, the average number of trials required to produce an acceptable result was 141, and the median was 133. The average number of threads required was 3.125, and the median was 3.

On culmination of the first thread search that is successful, the supervisory routine invokes up to two costate-rate adaptation search cycles (a maximum of seven predictions) performed using the algorithm described hereafter. If none of the available threads reaches an acceptable solution (which never occurred in the simulations performed), the supervisory routine selects the best result from among the multiple threads and proceeds with costate-rate adaptation. If a solution after adaptation remains inadequate, reinitialization is performed. Meanwhile, the maneuver starts with the best available solution as an interim guide.

For some applications, scoring should be based on $|x_e|$ and/or $|u_e|$ in addition to or in place of $|h_e|$ and $|v_e|$. More search trials may be needed if the number of participating final states is increased. Specification of only final altitude and vertical velocity does not impose uniqueness on the associated initial costate vector, partly because differently shaped trajectories can null a function of h_e and v_e. The additional $m_s - m_f$ penalty contributes to (but does not assure) uniqueness. It is not a significant retardant of search convergence and has obvious merit from an operational standpoint. Unique solutions for the initial costate vector are more the exception than the rule. It is not unusual to find different costate vectors that produce trajectories almost indistinguishable from one another. In other words, there are often multiple modes of acceptable quality in the search space, which improves the odds of finding a suitable mode.

The perimeter Lagrange constants K_1 and K_2 were 1.0 and 0.2, respectively, in all of the Fig. 1 searches and in the trajectory simulations presented in Sec. V. The setting of K_2 had a slight influence on the rate of fuel consumption, which tended to increase for values of K_2 larger and smaller than 0.2. Also, fuel consumption was less predictable for other settings of K_2.

The costate-rate adaptation that completed the initialization search readily compensated for residual predicted $|h_e|$ and $|v_e|$ values less than 10.0 m and 0.50 m/s (convergence acceptance levels for the random search threads). The 40 independent initializations (Fig. 1) had the following statistics for predictions by the costate initialization main search (before costate-rate adaptation)

$$h_e \text{ min} = -9.48 \text{ m}, \qquad v_e \text{ min} = -0.499 \text{ m/s}$$

$$h_e \text{ max} = 9.99 \text{ m}, \qquad v_e \text{ max} = 0.496 \text{ m/s}$$

$$h_e \text{ mean} = 0.16 \text{ m}, \qquad v_e \text{ mean} = -0.024 \text{ m/s}$$

$$h_e \text{ standard deviation} = 5.54 \text{ m}$$

$$v_e \text{ standard deviation} = 0.323 \text{ m/s}$$

and for predictions after costate-rate adaptation

$$h_e \text{ min} = -0.98 \text{ m}, \qquad v_e \text{ min} = -0.039 \text{ m/s}$$

$$h_e \text{ max} = 0.92 \text{ m}, \qquad v_e \text{ max} = 0.099 \text{ m/s}$$

$$h_e \text{mean} = -0.13 \text{ m}, \qquad v_e \text{ mean} = 0.003 \text{ m/s}$$

$$h_e \text{ standard deviation} = 0.66 \text{ m}$$

$$v_e \text{ standard deviation} = 0.022 \text{ m/s}.$$

B. Costate-Rate Adaptation

Costate-rate adaptation completes the initialization search and may also be used to provide midmaneuver compensation for small stochastic disturbances and/or identified changes in system parameters. Thus, if valid new estimates of parameters are obtained during a maneuver, a revised optimum path to go can be computed. In particular, adaptation is appropriate for impairments, if identifiable, in vehicle maneuvering capabilities (generally related to C_A, C_{N_α}, m, $T_{\max}$, and $T_{\min}$).

It has been found that adjustments of λ_{1_f} and λ_{2_f} are sufficient for costate-rate adaptation. Adjusted values of $\dot{\lambda}_1$ and $\dot{\lambda}_2$ are readily found at an adaptation time t_a knowing λ_1 and λ_2 at t_a and t_f. The search space for costate-rate adaptation can be regarded as unimodal for the scale of adjustments needed. A bivariate Newton search is suitable.

For small corrections in predicted final errors, h_e and v_e, and small perturbations in λ_{1_f} and λ_{2_f}, one has the first-order approximation

$$\begin{bmatrix} \delta h_f \\ \delta v_f \end{bmatrix} = -\begin{bmatrix} h_e \\ v_e \end{bmatrix} = \begin{bmatrix} a_{11} & a_{12} \\ a_{21} & a_{22} \end{bmatrix} \begin{bmatrix} \delta\lambda_{1_f} \\ \delta\lambda_{2_f} \end{bmatrix} \tag{96}$$

wherein

$$a_{11} = \frac{\partial h_f}{\partial \delta\lambda_{1_f}}, \qquad a_{12} = \frac{\partial h_f}{\partial \delta\lambda_{2_f}}$$

$$a_{21} = \frac{\partial v_f}{\partial \delta\lambda_{1_f}}, \qquad a_{22} = \frac{\partial v_f}{\partial \delta\lambda_{2_f}} \tag{97}$$

The inverse of Eq. (96) may be written in a modified form,

$$\delta\lambda_{1_f} = K(a_{22}\delta h_f - a_{12}\delta v_f)/D \tag{98}$$

$$\delta\lambda_{2_f} = K(a_{11}\delta v_f - a_{21}\delta h_f)/D \tag{99}$$

in which K is an adaptive gain factor (discussed hereafter) and $D = a_{11}a_{22} - a_{12}a_{21}$.

The sensitivity coefficients $a_{11}, \ldots, a_{22}$ are estimated at the time of adaptation t_a via a sequence of three predictions: First, a reference prediction of the pair $h_f^{(0)}$ and $v_f^{(0)}$ is computed using the prior best to date costate values $\lambda_{1_f}^{(0)}$ and $\lambda_{2_f}^{(0)}$. Second, $h_f^{(1)}$ and $v_f^{(1)}$ are predicted using $\lambda_{1_f}^{(1)} = \lambda_{1_f}^{(0)} + \delta\lambda_{1_f}$ and $\lambda_{2_f}^{(1)} = \lambda_{2_f}^{(0)}$. Third, $h_f^{(2)}$ and $v_f^{(2)}$ are predicted using $\lambda_{1_f}^{(2)} = \lambda_{1_f}^{(0)}$ and $\lambda_{2_f}^{(2)} = \lambda_{2_f}^{(0)} + \delta\lambda_{2_f}$. When $\delta\lambda_{1_f}$ and $\delta\lambda_{2_f}$ are small, such as $\delta\lambda_{1_f} = 0.001\lambda_{1_f}$, and $\delta\lambda_{2_f} = 0.001\lambda_{2_f}$, the estimates become

$$a_{11} = \left[h_f^{(1)} - h_f^{(0)}\right]\Big/\delta\lambda_{1_f}, \qquad a_{12} = \left[h_f^{(2)} - h_f^{(0)}\right]\Big/\delta\lambda_{2_f}$$

$$a_{21} = \left[v_f^{(1)} - v_f^{(0)}\right]\Big/\delta\lambda_{1_f}, \qquad a_{22} = \left[v_f^{(2)} - v_f^{(0)}\right]\Big/\delta\lambda_{2_f} \tag{100}$$

On convergence of the λ_{1_f} and λ_{2_f} estimates

$$\dot{\lambda}_{1_a} = \left(\lambda_{1_f} - \lambda_{1_a}\right)\Big/(t_f - t_a) \tag{101}$$

$$\dot{\lambda}_{2_a} = \left(\lambda_{2_f} - \lambda_{2_a}\right)\Big/(t_f - t_a) \tag{102}$$

In adjusting costate rates, the costates remain continuous.

To rule out premature termination of the predicted trajectory, predicted final error in time $(t_f)_e$ is also defined. For the results of a given search iteration to be accepted, predicted errors must not fail the following rejection test

$$(|h_e| > |h_e|_{\text{CB}} \quad \text{and} \quad |h_e| > |h_e|_{\max}) \quad \text{or}$$

$$(|v_e| > |v_e|_{\text{CB}} \quad \text{and} \quad |v_e| > |v_e|_{\max}) \quad \text{or}$$

$$|(t_f)_e/(t_f - t_a)| > 0.001 \tag{103}$$

The final values acceptability criterion used for costate-rate adaptation is $|h_e|_{\max} < 1.0$ m and $|v_e|_{\max} < 0.1$ m/s.

If the reference prediction, computed with a nominal 0.1-s integration interval at the start of a given adaptation search, is found acceptable in terms of the rejection test, it is recomputed using the 0.01-s integration interval (for high accuracy in propagating the solution forward) and the search is concluded. Otherwise (except for completion of initialization searches) the λ_{1_f} and λ_{2_f} search automatically performs a maximum of three cycles having three predictions per cycle, plus (after the third cycle) a concluding high-accuracy prediction. Thus, there are one, four, or seven predictions, depending on satisfaction of the adaptation acceptability criterion,

of which only one uses the 0.01-s integration interval. In flight, the costate-rate adaptation may be performed as often as necessary to maintain trajectory integrity, except that it should not be invoked in the last several seconds of a maneuver. Costate-rate adaptation nominally proceeds at intervals of $\Delta t_a = 1.0 + 0.005 t_{go}$ until $t_{go} < 20$ s, when the rates are frozen. After identification of vehicle parameter change, the interval is $\Delta t_a = 1.0$ s within the given maneuver.

K in the numerator factor of Eqs. (99) and (100) is a variable step-size factor used to improve search convergence. At the start of each adaptation process (comprising a maximum of three cycles), K is set to 0.77. If the cycle is successful vis-à-vis the test in conditions (103), K for the next cycle becomes 1.10; however, if the cycle is unsuccessful, K becomes a normally distributed random number having a mean value of 0.77 and standard deviation of 0.4.

V. Simulation Properties and Results

A. Simulation Properties

Nominal characteristics of a simulated notional unmanned aerial vehicle (UAV) are listed in the Appendix. The trajectory simulations for this vehicle employed fourth-order Runge–Kutta integration of the equations of motion. Integration time steps of 0.1 s were used for trajectory shooting and 0.01 s for refined calculations. Comparisons between results obtained with 0.1-s steps and steps as small as 0.001 s indicate that integration accuracy with the 0.1-s steps was better than 1.0 m in final altitude and 0.2 m/s in final vertical velocity for maneuvers of 1000-s duration. Accuracy with 0.01-s steps was effectively the same as that obtained with 0.001-s steps.

All simulations were conducted with $\Lambda_1 = 0$, $\sigma_1 = \sigma_2 = 1$, $K_1 = 1.0$, and $K_2 = 0.2$. All trajectories began with the UAV in horizontal flight trimmed for minimum steady-state thrust required, that is, with V_0, α_0, and T_0 determined from Eqs. (15–17) for given h_0, m_0, and γ_0. The vehicle was caused to remain in this trimmed initial flight for 5.0 s before starting its maneuver to allow for costate initialization. Trajectories were simulated with total durations of 600, 900, and 1200 s; thus, the allotted time for initialization computations was between 0.4 and 0.8% of total maneuver duration. T_{tr} and α_{tr} for all simulations were computed from Eqs. (19) and (18), which pertain to trim at minimum steady-state thrust required at the local values of V, h, m, and γ, all of which usually varied along the extremal paths.

In principle, initialization is predicated on estimates of states that will exist at t_s. (Here, the state estimation process was assumed to be error free.) Costate-rate adaptation began 5.0 s after an impairment, allowing time to estimate changes in parameter values. Costate-rate adaptation was simulated in all trajectories using a varying interval between adjustments of $\Delta t_a = 1.0 + 0.005 t_{go}$ s, except following identified parameter impairment(s), when $\Delta t_a = 1.0$ s was used after new parameter values became known. [In the absence of disturbances (not simulated here) and impairments, the postinitialization costate-rate adaptation had no significant effect.] Adaptation was always frozen at $t_{go} = 20$ s. A delay of 5.0 s was provided following vehicle in-flight parameter changes to allow time for parameter detection and estimation before costate-rate adaptation. (No processes were simulated for detection and estimation of parameter changes.)

B. Simulation Results

TPBV optimum trajectory simulation results are presented hereafter in the following categories: 1) ascents from 2000 to 6000 m with maneuver durations of 600, 900, and 1200 s; 2) descents from 6000 m to 2000 m with maneuver durations of 600, 900, and 1200 s; and 3) costate-rate adaptation for identified changes in vehicle aerodynamic parameters.

Figure 2 shows altitude profiles for representative ascent and descent trajectories.

Figures 3 and 4 accompany the 600-s ascent trajectory of Fig. 2 and show V, γ, α, and T vs time.

Figures 5 and 6 accompany the 600-s descent trajectory of Fig. 2 and show V, γ, α, and T vs time. Note the action of the $T_{min} =$ 2000 N limit on thrust (dictated by presumed engine flame-out below this limit). Mathematically, zero would be a preferable lower limit for descent thrust. (In extreme maneuvers a negative thrust

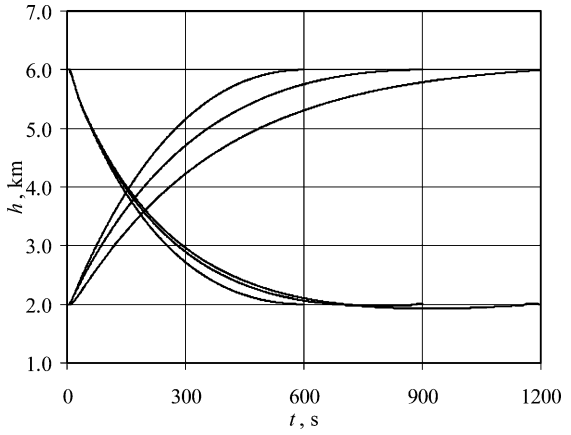

Fig. 2 Altitude profiles for 600-, 900-, and 1200-s ascent and descent maneuvers.

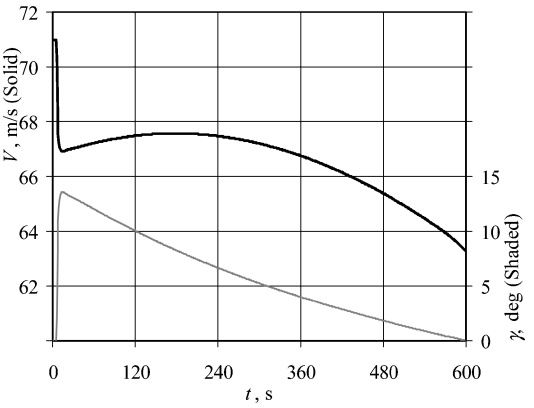

Fig. 3 V and γ profiles for 600-s ascent maneuver.

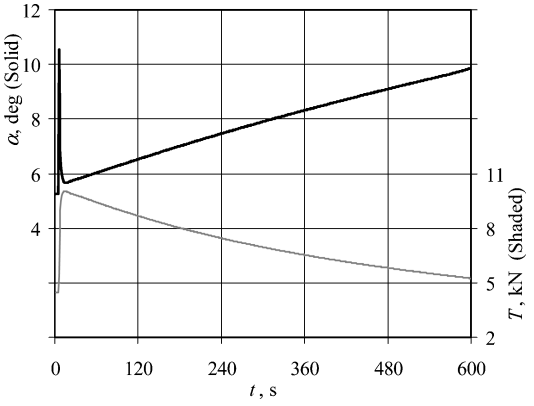

Fig. 4 α and T profiles for 600-s ascent maneuver.

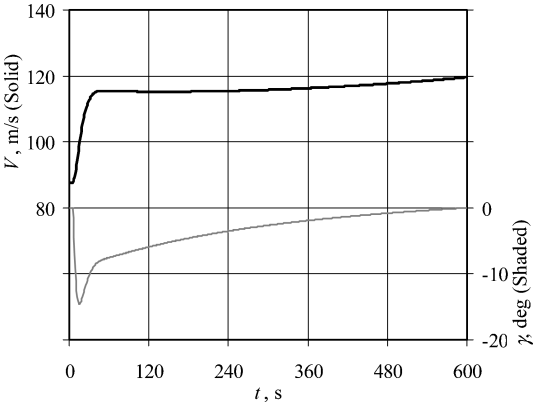

Fig. 5 V and γ profiles for 600-s descent maneuver.

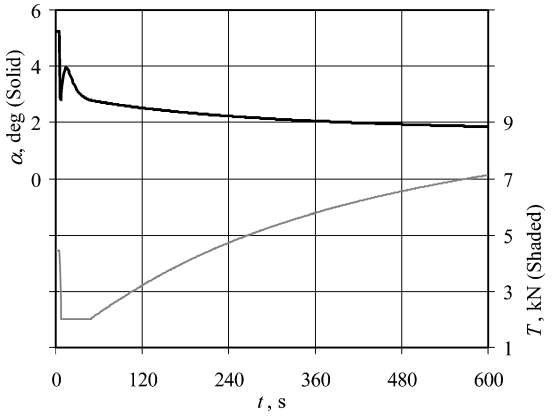

Fig. 6 α and T profiles for 600-s descent maneuver.

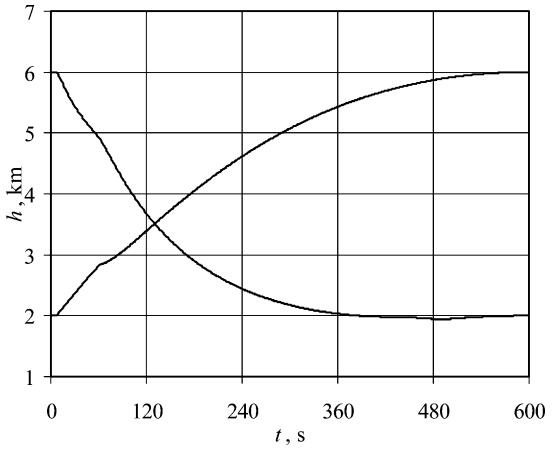

Fig. 7 Costate-rate adaptation: altitude profiles with parameter impairments at 60 s.

would be preferred by the variational solution.) A small, temporary undershoot of h_f (seen in Fig. 2) is an indirect consequence of the $T_{\min}$ limit.

Figures 4 and 6 show significant α and T changes in the interval between 5.0 and 10.0 s following inception of the maneuvers. At 5.0 s, the initialization search releases its costate solution, and the variational command functions react immediately. The α and T responses to command changes are rate limited (see the Appendix), but on the compressed timescale of the graphs these responses appear to be instantaneous. (A more detailed portrayal of initial transient responses follows.)

Figures 7–9 pertain to a study of costate-rate adaptation used to compensate for abrupt in-flight degradation of C_A and C_{N_α}. (It is assumed that changes in these parameters can be detected and identified numerically.) As mentioned earlier a 5.0-s delay in starting the costate-rate adaptation was simulated to allow time for estimation of the values of changed parameters, and, subsequently, adjusted costate rates were computed once per second until $t_{\text{go}} < 20$ s.

Figure 7 shows the altitude profiles of an impaired vehicle 600-s ascent from 2000 to 6000 m and an impaired vehicle descent of the same duration from 6000 to 2000 m. During the ascent, C_A was changed abruptly at 60.0 s from 0.025 to 0.0325, and, simultaneously, C_{N_α} was changed from 3.0 to 2.1, that is, 30% impairments were inserted. During the descent, C_A changed abruptly at 60.0 s from 0.025 to 0.030, and simultaneously, C_{N_α} was changed from 3.0 to 2.4. (In the descent case, 20% impairments were used because the vehicle could not perform its intended descent maneuver with 30% impairments when subject to the $T_{\min} = 2000$ N limit.)

Figure 8 shows the α and T commands for the first 120 s of the 600-s ascent maneuver of Fig. 7. The postinitialization and postimpairment transients are evident. Figure 9 shows the λ_1 and λ_2 behavior for the same trajectory. Note that the costate rates were constants from initialization (at 5.0 s) until the time of impairment induced

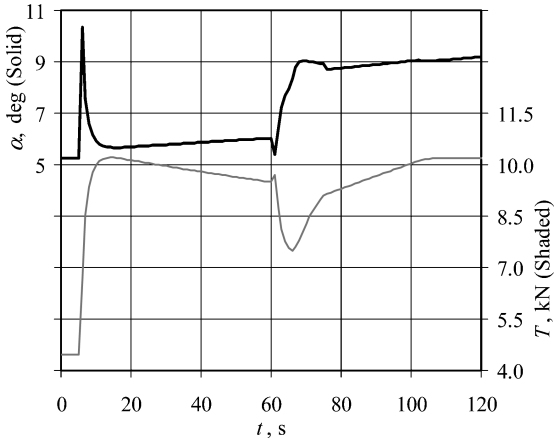

Fig. 8 Costate-rate adaptation: α and T with parameter impairments at 60 s.

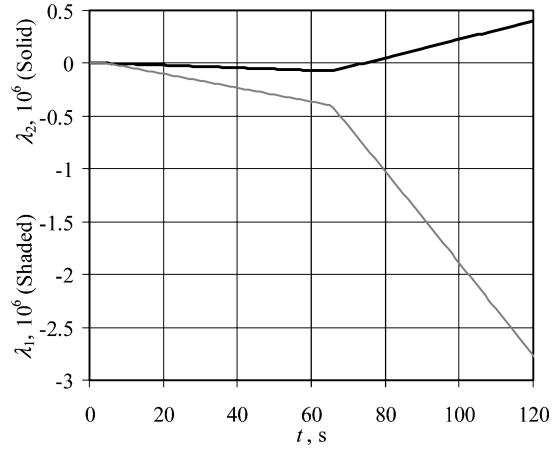

Fig. 9 Costate-rate adaptation: costates with parameter impairments at 60 s.

adaptation (65.0 s), then changed in the course of costate-rate adjustments at 1.0-s intervals.

VI. Discussion

The primary goal of the investigation described in this paper is realization of an improved indirect method for air-vehicle TPBV trajectory optimization. Prior work in this area has been hindered by convergence problems associated with costate initialization searches. These problems have arisen because of the following related factors:

1) Costate instability can radically reduce the radius of search convergence, producing attendant difficulty in searching and potentially creating chaotic system behavior arising from small disturbances and/or small errors in system models.

2) The costate initialization search must contend with complex multimodal search spaces.

3) Trajectory shooting for direct and indirect optimization methods is sensitive to errors in system dynamic models. For closed-loop guidance, both of these methods require processes for in-flight parameter change detection and parameter estimation and are potentially sensitive to unknown quasi-steady winds.

The approach offered in this paper addresses factors 1 and 2 with a degree of success. Nevertheless, there are several areas within this approach that need further investigation. Development of capabilities for three-dimensional solutions will be important, including solutions for motion relative to a rotating Earth. TPBV trajectories that satisfy all components of the final-boundary state vector are needed, and solutions when final states are prescribed via nonlinear functions of state and time will be required for some applications.

There is a subtle topic that also needs attention. The present approach employs an iterative trim solution for α and T [Eqs. (18) and (19)] that accepts externally supplied values of u and v (in the form

of V and γ). Because x_f and u_f are not specified for the costate initialization and costate-rate adaptation, optimum trajectories are free to reach the final boundary with any velocity above stalling speed. When x_f and u_f are not prescribed, it may be desirable to use a trim solution that solves for V [such as iteration of Eqs. (15–17)], so that final velocity is more tightly controlled.

Identification of vehicle parameter values and quasi-steady winds are vital for predictive initialization and adaptation processes. In-flight identification of parameters will be needed for closed-loop guidance predicated on the proposed method. If winds and air density are known, aerocoefficients are not difficult to identify. However, the simultaneous solution for vehicle aerocharacteristics and winds is ill conditioned and requires special care. Candidate techniques include model matching[17] and modified sequential least squares.[25] These topics have not been investigated in the present study.

VII. Conclusions

For a significant class of integral performance indices, the E–L necessary conditions of the calculus of variations require that the rates of change of costates be constant between points of discontinuity in the system dynamic model. With constant costate rates, costate initialization searches benefit from increased radii of convergence and simplified propagation of costates between boundaries. Although the search performance response surfaces remain multimodal, it is feasible to use arbitrary first iterates in a probabilistically controlled, multiple-thread, costate search algorithm for initializing air-vehicle TPBV optimum trajectories. Consequently, collocated analytical solutions, polynomial networks, and/or neural models are not required to seed the solution. Costate-rate adaptation provides a simple tool for solution refinement at the end of the initialization search and for identified subsequent changes in system parameters.

Appendix: Nominal Parameter Values of Notional UAV

The following nominal parameter values are assumed for a notional unimpaired unmanned aerial vehicle similar to the X-47A (Ref. 26):

$$m_i = 2000{-}3000 \text{ kg, depending on fuel and payload status}$$

$$\dot{m}_T = -6 \times 10^{-6} \text{ kg/s/N}, \qquad T_{\min} = 2000 \text{ N (203.9 kgf)}$$

$$T_{\max} = 20,000 \text{ N (2039 kgf)}, \qquad |\dot{T}|_{\max} = 1000 \text{ N/s}$$

$$C_A = 0.025, \qquad C_{N_\alpha} = 3.0/\text{rad}, \qquad S = 35 \text{ m}^2$$

$$|\alpha|_{\max} = 30 \text{ deg}, \qquad |\dot{\alpha}|_{\max} = 2.0 \text{ deg/s}$$

At a nominal altitude of 6000 m, the notional UAV has a minimum required thrust for trim in steady level flight of 4464 N (455.2 kgf), for which α_{tr} is 0.09167 rad (5.252 deg) and V_{tr} is 87.69 m/s.

Acknowledgments

The authors thank Andrew R. Barron of Yale University for encouraging renewed attention to trajectory performance criteria. Numerous helpful comments from the associate editor and reviewers of this paper are gratefully acknowledged.

References

[1]Barron, R., Mucciardi, A., Cook, F., Craig, J., and Barron, A., "Adaptive Learning Networks: Development and Application in the United States of Algorithms Related to GMDH," *Self-Organizing Methods in Modeling: GMDH Type Algorithms*, edited by S. J. Farlow, Marcel Dekker, New York, 1984, pp. 25–65.

[2]Barron, R. L., and Abbott, D. W., "Use of Polynomial Networks in Optimum Real-Time, Two-Point Boundary-Value Guidance of Tactical Weapons," *Proceedings of 1988 Military Computing Conference*, 1988.

[3]Barron, A. R., and Barron, R. L., "Statistical Learning Networks: A Unifying View," *Proceedings of the 20th Symposium on the Interface*, Computing Science and Statistics, edited by E. Wegman, American Statistical Association, Alexandria, VA, 1988, pp. 192–203.

[4]Ward, D., "Generalized Networks for Complex Function Modeling," *Proceedings of IEEE Systems, Man, and Cybernetics Conference*, Inst. of Electrical and Electronics Engineers, Piscataway, NJ, 1994.

[5]Ward, D., Monaco, J., and Schierman, J., "Reconfigurable Control for VTOL UAV Shipboard Landing," AIAA Paper 99-4015, Aug. 1999.

[6]Schierman, J. D., Ward, D. G., Hull, J. R., Ghandi, N., Oppenheimer, M. W., and Doman, D. B., "Integrated Adaptive Guidance and Control for Reentry Vehicles with Flight-Test Results," *Journal of Guidance, Control, and Dynamics*, Vol. 27, No. 6, 2004, pp. 975–988.

[7]Bulirsch, R., Montrone, F., and Pesche, H., "Abort Landing in the Presence of a Windshear as a Minimax Optimal Control Problem, Part 2: Multiple Shooting and Homotopy," *Journal of Optimization Theory and Applications*, Vol. 70, Aug. 1991, pp. 223–254.

[8]Leung, M. S. K., and Calise, A. J., "Hybrid Approach to Near-Optimal Launch Vehicle Guidance," *Journal of Guidance, Control, and Dynamics*, Vol. 17, No. 5, 1994, pp. 881–888.

[9]Calise, A. J., Melamed, N., and Lee, S., "Design and Evaluation of a Three-Dimensional Optimal Ascent Guidance Algorithm," *Journal of Guidance, Control, and Dynamics*, Vol. 21, No. 6, 1998, pp. 867–875.

[10]Gath, P. F., and Calise, A. J., "Optimization of Launch Vehicle Ascent Trajectories with Path Constraints and Coast Arcs," *Journal of Guidance, Control, and Dynamics*, Vol. 24, No. 2, 2001, pp. 296–304.

[11]Dukeman, G. A., "Atmospheric Ascent Guidance for Rocket-Powered Launch Vehicles," AIAA Paper 2002-4559, Aug. 2002.

[12]Lu, P., Sun, H., and Tsai, B., "Closed-Loop Endoatmospheric Ascent Guidance," *Journal of Guidance, Control, and Dynamics*, Vol. 26, No. 2, 2003, pp. 283–294.

[13]Calise, A. J., and Brandt, N., "Generation of Launch Vehicle Abort Trajectories Using a Hybrid Optimization Method," *Journal of Guidance, Control, and Dynamics*, Vol. 27, No. 6, 2004, pp. 930–937.

[14]Barron, R. L., and Chick, C. M., III, "Stabilization of Optimum Trajectory Costate Differential Equations," *Journal of Guidance, Control, and Dynamics*, Vol. 26, No. 4, 2003, pp. 665–668.

[15]Matyas, J., "Random Optimization," *Automation and Remote Control*, Vol. 26, No. 2, 1965, pp. 244–251.

[16]Rastrigin, L. A., *Random Search in Problems of Optimization of Multiparameter Systems*, Zinatne, Riga, U.S.S.R., 1965 (in Russian); English translation by U.S. Air Force Systems Command, Foreign Technology Div., Wright–Patterson Air Force Base, OH, 1967.

[17]Barron, R. L., "Inference of Vehicle and Atmosphere Parameters from Free-Flight Motions," *Journal of Spacecraft and Rockets,* Vol. 6, No. 6, 1969, pp. 641–648.

[18]Devroye, L., *A Bibliography on Random Search*, School of Computer Science, McGill Univ., Montreal, 1979.

[19]Betts, J. T., "Survey of Numerical Methods for Trajectory Optimization," *Journal of Guidance, Control, and Dynamics*, Vol. 21, No. 2, 1998, pp. 193–205.

[20]Wuerl, A., Crain, T., and Braden, E., "Genetic Algorithm and Calculus of Variations-Based Trajectory Optimization Technique," *Journal of Spacecraft and Rockets*, Vol. 40, No. 6, 2003, pp. 882–888.

[21]Kirk, D. E., *Optimal Control Theory: An Introduction*, Prentice–Hall, Englewood Cliffs, NJ, 1970, p. 251.

[22]"Recommended Practice for Atmospheric and Space Flight Vehicle Coordinate Systems," American National Standards Inst./AIAA Rept. R-04-1992, Feb. 1992.

[23]Barron, R. L., "Trigonometric Models for Large-Angle Aerodynamic Force Coefficients," *Journal of Guidance, Control, and Dynamics*, Vol. 26, No. 5, 2003, pp. 825–827.

[24]Press, W. H., Teukolsky, S. A., Vetterling, W. T., and Flannery, B. P., *Numerical Recipes in C*, Cambridge Univ. Press, Cambridge, England, U.K., 1992, pp. 379–383.

[25]Ward, D. G., Monaco, J. F., and Bodson, M., "Development and Flight Testing of a Parameter Identification Algorithm for Reconfigurable Control," *Journal of Guidance, Control, and Dynamics*, Vol. 21, No. 6, 1998, pp. 948–956.

[26]Croft, J., "Pegasus: UCAVS Look Seaward," *Aerospace America*, Vol. 41, No. 9, 2003, pp. 36–42.